Visualization of human retinal capillary networks: A comparison of intensity, speckle-variance and phase-variance optical coherence tomography

Dae Yu Kim,[1,2]* Jeff Fingler,[3] John S. Werner,[1,2] Daniel M. Schwartz,[4]
Scott E. Fraser,[3] and Robert J. Zawadzki[2]

[1]Depts. of Biomedical Engineering and [2]Ophthalmology & Vision Science,
University of California Davis, Davis, CA,
[3]Dept. of Biology, California Institute of Technology, Pasadena, CA,
[4]Dept. of Ophthalmology, University of California San Francisco, San Francisco, CA;

ABSTRACT

We evaluate methods to visualize human retinal micro-circulation *in vivo* by standard intensity-based optical coherence tomography (OCT), speckle-variance optical coherence tomography (svOCT), and phase-variance optical coherence tomography (pvOCT). *En face* projection views created from the same volumetric data set of the human retina using all three data processing methods are created and compared. Additionally we used support vector machine (SVM) based semi-automatic segmentation to generate *en face* projection views of individual retinal layers. The layers include: first, the whole inner retina (from the nerve fiber layer to the outer nuclear layer), and second, from the ganglion cell layer to the outer nuclear layer. Finally, we compare the retinal vasculature images processed from the three OCT techniques and fluorescein angiography (FA).

Keywords: Optical coherence tomography; Phase contrast technique; Imaging system; Medical optics instrumentation

* dyukim@ucdavis.edu; phone 1 916 734-5839; fax 1 916 734-4543; http://vsri.ucdavis.edu/

1. INTRODUCTION

Vasculature imaging in the retina is routinely used to diagnose retinal vascular diseases and to monitor treatment progress in clinical settings. Currently, fundus fluorescein angiography (FA) is the most widely used technique and also considered a gold standard for visualization of the retinal vasculature. Several methods implementing optical coherence tomography (OCT) [1,2] for imaging and visualization of retinal perfusion maps have been implemented. These include Doppler OCT [3-5], optical micro-angiography [6], joint spectral and time-domain optical coherence tomography [7] and dual-beam Doppler OCT [8,9]. Phase-variance OCT (pvOCT) [10,11] used in this study produces high contrast microcirculation imaging of the retina of healthy and diseased subjects within just a few seconds of acquisition time.

In addition to Doppler and phase-based methods used to visualize retinal perfusion maps, the parafoveal capillary network reconstructed from standard OCT intensity images was presented with a fractal dimension analysis [12]. Unlike phase processing methods including Doppler and phase-variance OCT, intensity-based methods allow simple acquisition and post-processing as well as fewer artifacts from sample motion and vessel shadows in the axial direction.

In this manuscript, we evaluate three OCT-based retinal vasculature imaging techniques used to enhance contrast, intensity-based averaging, speckle-variance, and phase-variance methods. *In vivo* human retinal OCT data are acquired at different retinal regions. A segmented volumetric data set is used to allow projection views of retinal perfusion from selected retinal layers.

2. METHODS

2.1 Experimental system, image acquisition and processing

Optical Coherence Tomography and Coherence Domain Optical Methods in Biomedicine XVI,
edited by Joseph A. Izatt, James G. Fujimoto, Valery V. Tuchin, Proc. of SPIE Vol. 8213, 821307

A detailed description of the experimental system is published elsewhere [11]. In short, we use a custom-built Fourier-domain OCT (Fd-OCT) system with a superluminescent diode (Superlum Ltd.) centered at 855nm and full width at half maximum (FWHM) of 75nm. The axial and lateral resolution of the system are ~4.5μm and ~15μm in the retina, respectively. The imaging beam power of the pupil is approximately 700μW. A custom-built spectrometer employs a CMOS (complementary metal-oxide-semiconductor) detector (spL4096-140km, Basler) operating at 125,000 lines/s using 2048 pixels. The spacing between consecutive A-scans and BM-scans for the 1.5x1.5mm^2 scanning scheme used for the data presented in this manuscript was 4μm.

Scanning protocols are based upon a series of BM-scans acquired across the fovea, with each BM-scan consisting of three cross-sectional images (B-scans) acquired in succession over the same scanning position (BM-scan). Two volumetric OCT data sets (1.5x1.5mm^2) were acquired from a healthy volunteer. The average intensity images, speckle-variance image processing [14], as well as phase-variance image processing [11] are calculated from each BM-scan as described by following equations.

$$Intensity\ \ Averaging = \frac{1}{N}\sum_{i=1}^{N} I_i(x,z) \tag{1}$$

$$Speckle\ \ Variance\ = \frac{1}{N}\sum_{i=1}^{N}[I_i(x,z) - \frac{1}{N}\sum_{i=1}^{N} I_i(x,z)]^2 \tag{2}$$

$$Phase\ Variance = \frac{1}{N-1}\sum_{i=1}^{N-1}[\Delta\varphi_i(x,z) - \frac{1}{N-1}\sum_{i=1}^{N-1}\Delta\varphi_i(x,z)]^2 \tag{3}$$

Here, $I_i(x,z)$ is the OCT intensity of the same location between consecutive B-scans in the B-scans at lateral location *x*, depth position *z*, and *i* is an index of the *i*-th B-scan within one BM-scan. $\Delta\varphi_i(x,z)$ is the phase difference between two consecutive B-scans.

A semi-automatic segmentation procedure [13] was implemented to separate the inner retina, from the nerve fiber layer (NFL) to the outer nuclear layer (ONL), on the volumetric data set. These data were processed by three different image-processing methods. Maximum intensity projection of the segmented data sets generates a gray-scale perfusion map of the inner retinal vessels. In the superficial retina, there is the NFL, the hyper-reflecting intensity signal region of OCT, which causes production of low-contrast vasculature imaging with the intensity-based processing methods. Thus, in order to separate the NFL from the other inner retinal layers, the semi-automatic segmentation program, implementing a support vector machine (SVM) algorithm [13], is used to generate two volumetric retinal layers, one from the NFL to the ONL and one from the ganglion cell layer (GCL) to the ONL. Figure 1 shows the result of the segmentation of the human inner retinal layers from a healthy volunteer. Figure 1 (a) shows an average intensity image composed of three successive B-scans from a single BM-scan. The size of the lateral scan is 1.5mm. The green-colored area of Figure 1 (b) indicates the segmented layers, from the GCL to the ONL.

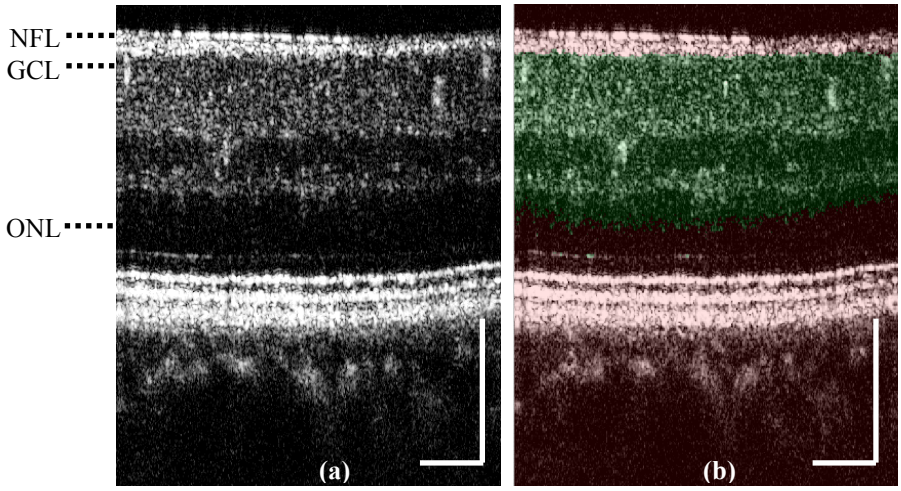

Figure 1. OCT B-scan images of the left eye from a healthy volunteer. The size of lateral scans is 1.5mm. (a) Averaged OCT intensity image from the BM-scan (three B-scans). (b) Segmentation (green color) from the GCL to the ONL with the averaged OCT intensity image (a). Scale bar: 250μm.

En face projection of OCT data sets generated by the intensity averaging, the speckle-variance, and the phase-variance methods produce a two-dimensional (2D) vasculature map. Furthermore, the fundus FA image of the same subject is used to analyze 2D perfusion maps showing inner retinal vasculature.

3. RESULTS

The fundus FA photo of this subject's left eye is shown in Figure 2 (a), magnified in the foveal region. The image size is 1.5 x 1.5mm^2 and was acquired with the Heidelberg Spectralis (HRA+OCT). Two-dimensional projection images generated by averaged intensity projection of the whole inner retina and the inner retina without the NFL are presented in Figure 2 (b) and (c), respectively. The perfusion map of Figure 2 (c), after removing the NFL, shows an enhanced-contrast of the vascular network compared to Figure 2 (b). Note that the bright spot (marked as red dotted circle) in the center of the FAZ in Figure 2 (b) and (c) is a back-reflection signal from the central fovea. Figure 2 (d) and (e) demonstrate the *en face* projection view achieved by the speckle-variance method segmented for the whole inner retina and the inner retina without the NFL, respectively. These two images, with and without the NFL, exhibit an almost identical perfusion map because of weak speckle-variance signal from the thin NFL. In addition, the images from the speckle-variance method demonstrate similar results of the projection view of the whole inner retina for phase-variance OCT shown in Figure 2 (f) excluding vertical stripes (marked as red arrows) at Figure 2 (d) and (e). This is because the phase-variance method allows removal of bulk motion artifacts unlike the speckle-variance method. All the reconstructed images correlate with the zoomed FA image shown in Figure 2 (a) with varying contrast of the capillaries.

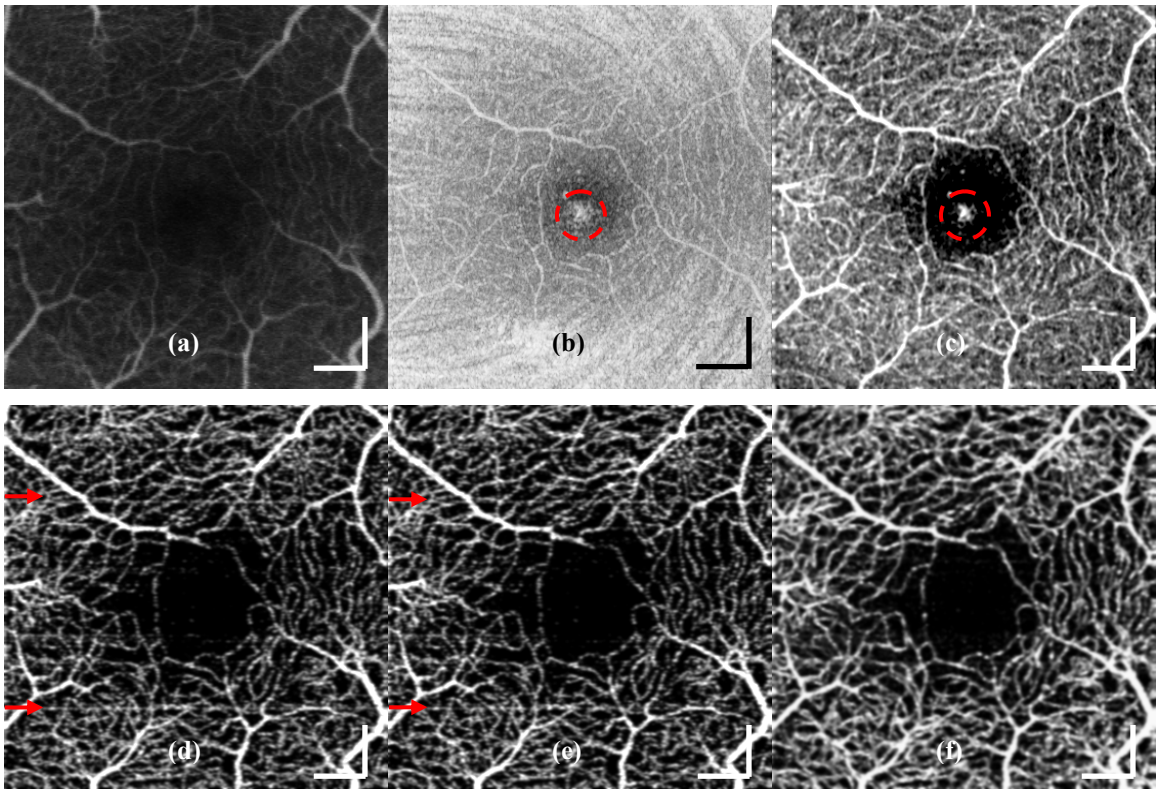

Figure 2. Retinal perfusion network of the foveal region, 1.5x1.5mm^2 area reconstructed from the same subject as Figure 1. (a) Fundus FA. (b) *En face* projection of OCT intensity average segmented from the NFL to the ONL, and (c) segmented from the GCL to the ONL. (d) *En face* speckle-variance images from the NFL to the ONL, and (e) from the GCL to the ONL. Red arrows mark position of bulk motions during acquisition. (f) *En face* visualization of pvOCT processed over the inner retina [15]. Scale bar: 300μm.

Figure 3 shows similar analyses of the OCT volumetric data sets acquired at approximately 8 degree nasal and 8 degree inferior retinal eccentricity. Note that *en face* projection of averaged OCT intensity cannot provide high-contrast for microcapillaries (diameter of 5~15μm) in this region. The larger diameter of capillaries located at the border between the NFL and GCL are present in both images of Figure 3 (b) and (c). Comparing between Figure 3 (d) and (f), the speckle-variance values from small capillaries are not sufficient to permit visualization of microcirculation in the whole inner retinal layers. One reason is that the svOCT has strong variance values from the thick bright NFL. In the thick hyper-scattering layer, not all the variance values are from the vasculature as shown in Figure 3 (b). Moreover, the method acquires weak variance values from microcapillaries underneath the bulky NFL due to the degraded OCT intensity signal of the microcapillaries in Figure 4 (a). This may cause only small OCT intensity differences between the inner retinal structures and capillaries in Figure 4 (b), resulting in loss of speckle-variance values. As a consequence, *en face* projection view generated from svOCT from the inner retina without NFL has missing small capillaries in the bottom part of Figure 3 (e). However, phase-variance OCT, in Figure 4 (c), shows microcirculation information as well as larger diameter vessels without this drawback as shown in Figure 3 (f).

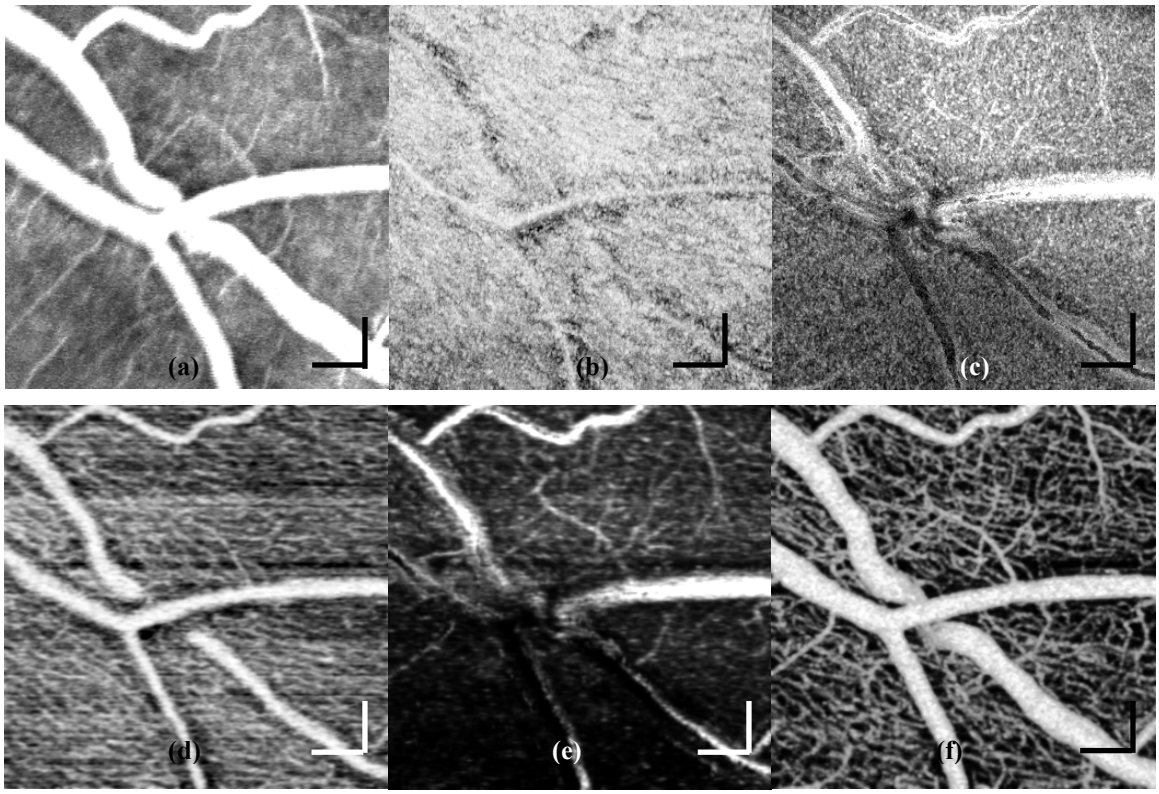

Figure 3. Retinal vascular network acquired at approximately 8 degree nasal and inferior retinal eccentricity (1.5x1.5mm^2) and taken from the same subject as Figures 1 and 2. (a) Fundus FA. (b) *En face* average OCT intensity projection from the inner retina, and (c) from the inner retina without NFL. (d) *En face* maximum intensity projection from the inner retina using speckle-variance OCT, and (e) *en face* maximum intensity projection from the inner retina without NFL using speckle-variance OCT. (f) *En face* maximum intensity projection from the inner retina using pvOCT [11]. Scale bar: 300μm.

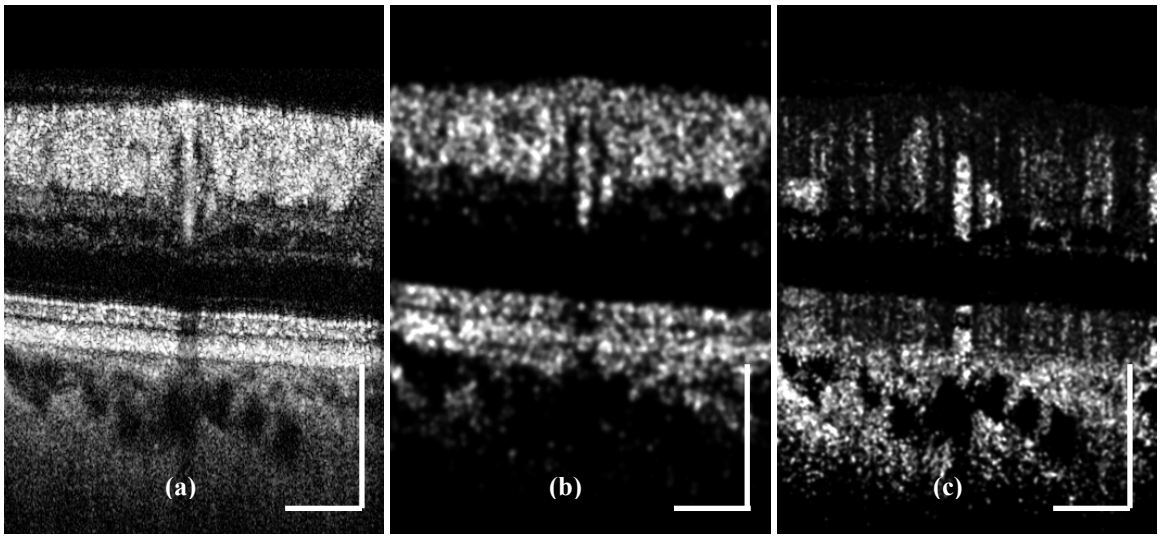

Figure 4. OCT retinal images from a single BM-scan (three B-scans at the same position). The processed images were acquired at the last B-scan of the volumetric data (1.5x1.5mm^2) used in Figure 3. (a) Average intensity image. (b) Speckle-variance image. (c) Phase-variance image. Scale bar: 300μm.

CONCLUSIONS

We demonstrate *en face* visualization of capillary network of the human fovea and the retina near the optic nerve head using OCT intensity averaging, speckle-variance OCT, and phase-variance OCT. The OCT intensity averaging method produces low-contrast images of the vascular network due to the bright NFL and inner retinal structures. The svOCT demonstrates similar perfusion maps with FA and pvOCT scanned over the central foveal region. However, speckle-variance values from the microcapillaries in the NFL and below the thick NFL are not dominant enough to allow reliable visualization of microcirculation. Unlike the OCT intensity-based processing methods, the pvOCT visualizes microcapillaries and larger vessels from the OCT scanned volumes without these limitations.

ACKNOWLEDGEMENTS

This research was partially supported by National Eye Institute (EY 014743), Research to Prevent Blindness (RPB), Beckman Institute, and That Man May See Foundation.

REFERENCES

1. D. Huang, E. A. Swanson, C. P. Lin, J. S. Schuman, W. G. Stinson, W. Chang, M. R. Hee, T. Flotte, K. Gregory, C. A. Puliafito, and J. G. Fujimoto, "Optical Coherence Tomography," Science 254, 1178-1181 (1991)
2. A. F. Fercher, C. K. Hitzenberger, W. Drexler, G. Kamp, and H. Sattmann "*In vivo* optical coherence tomography," Am. J. Ophthalmol. 116, 113-114 (1993)
3. L. Yu and, Z. Chen, "Doppler variance imaging for three-dimensional retina and choroid angiography," J. Biomed. Opt., Vol. **15**, 016029 (2010)
4. T. Schmoll, C. Kolbitsch, and R. A. Leitgeb, "Ultra-high-speed volumetric tomography of human retinal blood flow," Opt. Express **17**, 4166-4176 (2009)
5. Y. Tao, K. Kennedy, and J. Izatt, "Velocity-resolved 3D retinal microvessel imaging using single-pass flow imaging spectral domain optical coherence tomography," Opt. Express **17**, 4177–4188 (2009)
6. L. An and R. K. Wang, "In vivo volumetric imaging of vascular perfusion within human retina and choroids with optical micro-angiography," Opt. Express **16**, 11438-11452 (2008)
7. A. Szkulmowska, M. Szkulmowski, D. Szlag, A. Kowalczyk, and M. Wojtkowski, "Three-dimensional quantitative imaging of retinal and choroidal blood flow velocity using joint spectral and time domain optical coherence tomography," Opt. Express **17**, 10584–10598 (2009)
8. S. Zotter, M. Pircher, T. Torzicky, M. Bonesi, E. Götzinger, R. A. Leitgeb, and C. K. Hitzenberger, "Visualization of microvasculature by dual-beam phase-resolved Doppler optical coherence tomography," Opt. Express **19**, 1217-1227 (2011)
9. S. Makita, F. Jaillon, M. Yamanari, M. Miura, and Y. Yasuno, "Comprehensive in vivo micro-vascular imaging of the human eye by dual-beam-scan Doppler optical coherence angiography," Opt. Express **19**, 1271-1283 (2011).
10. J. Fingler, R. J. Zawadzki, J. S. Werner, D. Schwartz, and S. E. Fraser, "Volumetric microvascular imaging of human retina using optical coherence tomography with a novel motion contrast technique," Opt. Express 17, 22190-22200 (2009)
11. D. Y. Kim, J. Fingler, J. S. Werner, D. M. Schwartz, S. E. Fraser, and R. J. Zawadzki, "In vivo volumetric imaging of human retinal circulation with phase-variance optical coherence tomography," Biomed. Opt. Express 2, 1504-1513 (2011)
12. T. Schmoll, A. S. G. Singh, C. Blatter, S. Schriefl, C. Ahlers, U. Schmidt-Erfurth, and R. A. Leitgeb, "Imaging of the parafoveal capillary network and its integrity analysis using fractal dimension," Biomed. Opt. Express 2, 1159-1168 (2011)
13. A. R. Fuller, R. J. Zawadzki, S. Choi, D. F. Wiley, J. S. Werner, and B. Hamann, "Segmentation of three-dimensional retinal image data," IEEE Trans. Vis. Comput. Graph. 13(6), 1719–1726 (2007)
14. A. Mariampillai, B. A. Standish, E. H. Moriyama, M. Khurana, N. R. Munce, M. K. K. Leung, J. Jiang, A. Cable, B. C. Wilson, I. A. Vitkin, and V. X. D. Yang, "Speckle variance detection of microvasculature using swept-source optical coherence tomography," Opt. Lett. **33**, 1530-1532 (2008)
15. D. Y. Kim, J. Fingler, R. J. Zawadzki, S. S. Park, L. S. Morse, D. M. Schwartz, S. E. Fraser, and J. S. Werner, " Noninvasive imaging of the foveal avascular zone with high-speed, phase-variance optical coherence tomography," Invest Ophthalmol Vis Sci. 53(1), 85-92 (2012)